

Insights into the Hydrothermal Stability of ZSM-5 under Relevant Biomass Conversion Reaction Conditions

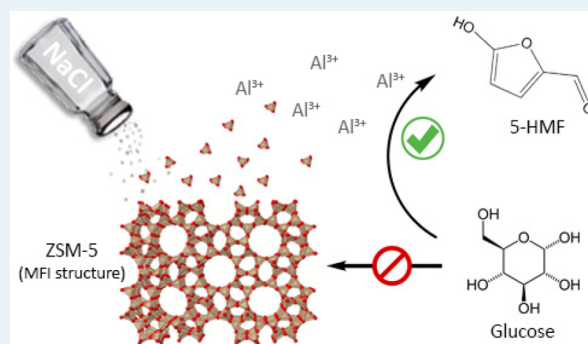
David W. Gardner,^{†,§} Jiajie Huo,^{†,‡,§} Thomas C. Hoff,^{†,§} Robert L. Johnson,^{†,‡} Brent H. Shanks,^{†,‡} and Jean-Philippe Tessonnier^{*,†,‡}

[†]Department of Chemical and Biological Engineering, Iowa State University, Ames, Iowa 50011, United States

[‡]NSF Engineering Research Center for Biorenewable Chemicals (CBiRC), Ames, Iowa 50011, United States

S Supporting Information

ABSTRACT: Zeolite catalysts used for the conversion of carbohydrates to renewable platform chemicals in the condensed phase are shown to be sensitive to the presence of inorganic salts which alter the zeolite surface chemistry. The presence of NaCl (0.07–37 wt %) enhances the hydrolysis of Si–O–Al bridges and the release of Al³⁺ species that catalyze the conversion of glucose through homogeneous catalytic processes and obscure the apparent reactivity of the zeolite catalyst.



KEYWORDS: biomass conversion, glucose, fructose, zeolite, ZSM-5, hydrothermal stability, hot liquid water, salt effects

The production of renewable chemicals from biomass-derived carbohydrates commonly takes place under hydrothermal conditions at temperatures between 100 and 200 °C.^{1–3} Typical oxide catalysts and catalyst supports, including silica, alumina, and zeolites, undergo phase transitions and partial dissolution under these severe conditions.^{4–11} The hydrothermal breakdown of mesoporous silica is dramatic as evidenced from the 90% loss of its surface area within 10 h at 200 °C.⁴ Hydrothermal degradation of γ -alumina is also rapid and is evident from the phase transition to hydrated boehmite under the same conditions.⁵ γ and β zeolites degrade through leaching and amorphization.^{7–12}

In the case of binary oxides (e.g., silica), dissolution occurs until reaching an equilibrium concentration of inorganic species in solution.¹³ At equilibrium, the rates for dissolution and deposition are equal, and both reactions take place simultaneously. Oxides can then undergo major changes in crystal size and structure under relatively mild conditions through dissolution–deposition. Small-angle neutron scattering (SANS) demonstrated that dissolution of SBA-15 in water at 115 °C starts in areas of positive curvature (e.g., at the pore mouth), and the dissolved silica diffuses deeper into the micropores where it is redeposited.^{6,13} Although not often used in catalysis, models that explain these phenomena have been developed by geochemists, and the key parameters that influence these transformations are known.^{13–16} The critical factors governing hydrothermal breakdown are the elemental composition of the oxide, its crystallographic structure, temperature, pH, and ionic strength of the solution.^{13–16}

Stability tests performed on oxide catalysts and catalyst supports were typically carried out in hot liquid water.^{1,4–7,10–13} Although this medium is relevant for the liquid-phase conversion of biomass, deionized water does not accurately model real reaction conditions, especially (i) for acid–base catalyzed reactions, (ii) when organic acids are formed under reaction conditions, (iii) when salts are present in the biomass feedstock or added to the process. Salts only represent about 1.5 wt % of dry biomass.¹⁷ Therefore, the effects of these inorganic compounds on heterogeneous catalysts is often overlooked, and experiments are performed under idealized conditions.

Here, we studied the effect of pH and salts on the activity and stability of ZSM-5 (MFI structure), the only zeolite that has been previously demonstrated to be stable in deionized water at 150 and 200 °C for more than 6 h.⁷ MFI-type zeolites recently gained increasing attention due to their superior catalytic performance for the conversion of cellulosic sugars.^{18–21} The purpose of this work is to provide further insights into the effect of pH and ionic strength of the reaction medium on the chemistry at the liquid–solid interface.

Protonic ZSM-5 with a Si/Al ratio of 11.5 (Zeolyst, CBV2314) was first tested for the biphasic dehydration of fructose to 5-hydroxymethylfurfural (HMF). Reaction conditions similar to those employed previously when testing β -zeolite,^{8,9} Sn- β ,²² and homogeneous acids were used for easier

Received: April 30, 2015

Revised: June 6, 2015

Published: June 15, 2015

Table 1. Reaction Conditions, Catalytic Results, and Post-Reaction ICP-MS Analysis Data for the Conversion of Glucose and Fructose to HMF

entry	catalyst	pH	NaCl concn (%)	reactant	Al in solution (ppm)	Si in solution (ppm)	conversion (%)	selectivity to HMF (%)
1	ZSM-5	2.5	37	fructose	91.3	84.5	100	81
2	ZSM-5	6.6	0	glucose	21.2	157.1	21	0
3	ZSM-5	2.5	0	glucose	40.1	154.2	27	0
4	ZSM-5	5.9	37	glucose	100.2	56.6	42	7
5	ZSM-5	2.5	37	glucose	99.7	97.2	63	33
6	filtered solution	2.5	37	glucose	86.1	103.1	86	52
7	ZSM-5	2.5	0.07	glucose	67.7	176.5	31	25
8	ZSM-5	2.5	0.18	glucose	114.2	197.9	60	18
9	no catalyst	2.5	37	glucose	0.8	8.6	15	0
10	ZSM-5, treated	2.5	37	glucose	70.0	/	81	40

All reactions were performed for 30 min at 170 °C in 10 mL thick-wall glass reactors under biphasic conditions. *sec*-Butyl phenol was used as the organic extracting phase. Entry 6 corresponds to the solution recovered after treating ZSM-5 in a 37 wt % NaCl solution at pH 2.5 for 30 min at 170 °C (Supporting Information). Entry 10 corresponds to ZSM-5 treated five successive times in a 37 wt % NaCl solution at pH 2.5 for 90 min at 170 °C (Supporting Information). The concentration of Si in solution was not measured for Entry 10.

comparison.^{23–28} Fructose and ZSM-5 catalyst were suspended in a 37 wt % NaCl aqueous solution (saturated under ambient conditions). *sec*-Butyl phenol was used as an immiscible organic phase to extract HMF (Supporting Information). The reaction was carried out in thick-wall glass reactors for 30 min at 170 °C. ZSM-5 led to 100% fructose conversion within 30 min at 170 °C with 81% selectivity to HMF, in good agreement with previous studies (Table 1).^{29,30} However, inductively coupled plasma mass spectrometry (ICP-MS) analysis of the solution revealed significant leaching of Si (84.5 ppm) and Al (91.3 ppm) from the solid catalyst within only 30 min. These concentrations are significant as they correspond to the dissolution of ~0.3 and ~3.7% of Si and Al initially present in the zeolite.

Al³⁺ is known to promote the acid-catalyzed hydrolysis of cellulose³¹ and the isomerization of glucose to fructose through Lewis acid-catalyzed intramolecular hydride shift.^{24,26,32} However, the catalytic activity of Al³⁺ varies with the structure of the hydrated species as determined by the solution conditions.^{26,32} We studied ZSM-5 for the cascade glucose isomerization-fructose dehydration reaction in order to assess the contribution of heterogeneous and homogeneous Al species to the observed activity. In addition, individual and synergistic effects of HCl and NaCl were studied by varying the composition of the aqueous phase (Table 1, Entries 2–5). As expected, ZSM-5 had no significant effect on the conversion of glucose to fructose and HMF when the reaction was carried out in the absence of NaCl and HCl. Glucose diffusion inside the 5.1–5.6 Å pores of the ZSM-5 is significantly hindered compared to β zeolite (5.6–6.7 Å)^{18,33,34} and carbohydrates can only react with active sites located on the outer surface or at pore rims.^{18,34} In contrast, a significant increase in catalytic activity was observed after adding HCl and NaCl, as evidenced by the change in color of the aqueous phase (Figure 1). Lowering the pH to 2.5 and saturating the solution with NaCl increased glucose conversion from 21 to 63% and HMF selectivity from 0 to 33% (Entries 2 and 5). ICP-MS analyses of the solutions after 30 min at 170 °C revealed that the concentrations of Si and Al species in solution varied with the composition of the aqueous phase (Table 1, Figure 1). The effect of NaCl was especially severe on Al leaching as 0.07% NaCl led to 67.7 ppm Al in solution.

Dry biomass contains about 1.5 wt % of inorganic salts with NaCl being the main contributor.^{17,35} We showed previously

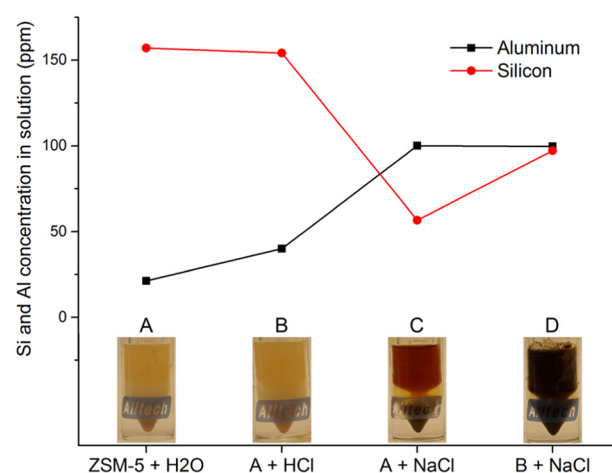


Figure 1. Influence of pH and NaCl on leaching and on the observed catalytic activity. Si and Al concentrations in solution were determined by ICP-MS. The insets show photos of the aqueous phases after 30 min reaction at 170 °C.

that Na⁺ ions can interfere when pyrolyzing cellulose at high temperature.³⁵ Na⁺ alters reaction pathways and modifies the product distribution. Therefore, experiments were carried out to determine if NaCl also influences the conversion of glucose in the liquid phase (Entry 9). NaCl was found to not significantly impact glucose conversion, thus demonstrating that Na⁺ does not play any direct role in the reaction. In addition, ICP-MS confirmed that Al and Si detected in the solution after reaction were not due to impurities in NaCl (Entry 9). Finally, we found a linear correlation between glucose conversion and the concentration of Al species in solution (Figure 2). However, at this point, it was unclear whether the detected Al species were the cause or the consequence of the observed catalytic activity. To address this question, ZSM-5 was treated under the same conditions without glucose (pH 2.5, 37 wt % NaCl, 170 °C, 30 min), and the aqueous phase was recovered by filtration (Supporting Information). The catalytic activity of the filtrate was then tested in the absence of ZSM-5 (Entry 6), and 86% conversion and 52% selectivity to HMF were achieved. This experiment confirms that Al species in solution present Lewis acid properties and that glucose is consumed through Lewis-acid

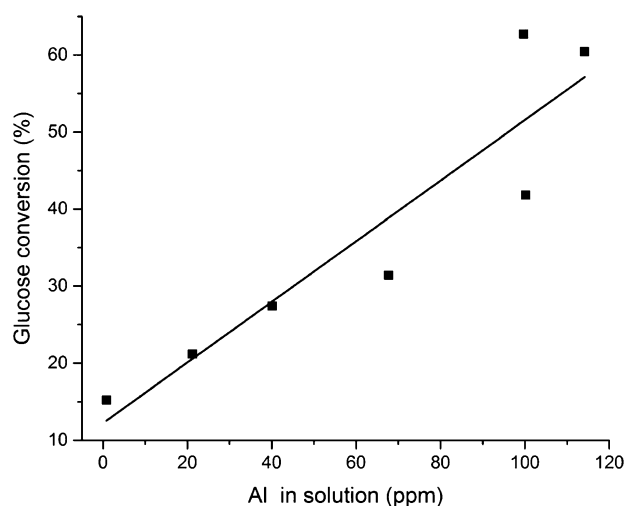


Figure 2. Correlation between the glucose converted after 30 min reaction at 170 °C and the concentration of leached Al species detected in the reacted aqueous phase.

catalyzed isomerization to fructose, followed by dehydration to HMF.

Further investigations were carried out on the reacted heterogeneous catalyst by X-ray diffraction (XRD) and on the resulting solution via ^{27}Al nuclear magnetic resonance (NMR) spectroscopy in order to better understand the dissolution mechanism, and understand the state of the Al leached into the solution. Diffractograms acquired for ZSM-5 samples before and after reaction using corundum as an internal standard for phase quantification revealed no significant difference in crystallinity (within 5% error, Figures 3). Therefore, dissolution

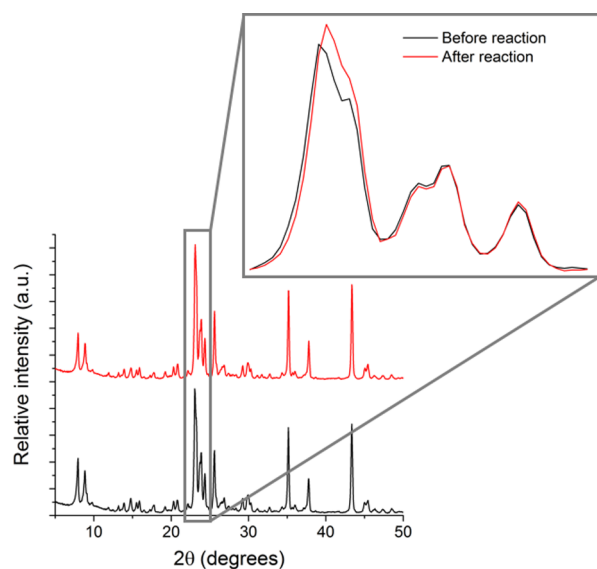


Figure 3. XRD patterns of ZSM-5 before and after a 30 min treatment at 170 °C in an acidic NaCl solution (37% NaCl, pH 2.5).

occurs primarily at amorphous or defective regions of the sample and the ZSM-5 crystal structure remains intact. In order to determine if the Al species in solution are fully dissolved ions or zeolite fragments (colloids), ^{27}Al NMR spectra were collected and then compared to spectra of standard solutions of both AlCl_3 (Figure 4) and $\text{Al}(\text{NO}_3)_3$ (Figure S1) containing Al^{3+} concentrations of 5000, 500, 250, and 100 ppm. Both

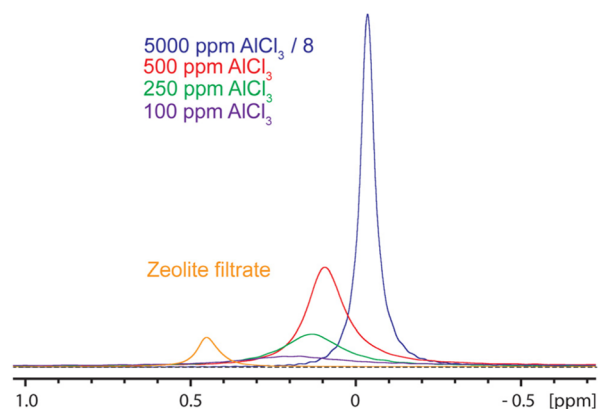


Figure 4. ^{27}Al NMR spectra the supernatant after reaction and standard solution containing 100, 250, 500, or 5000 ppm AlCl_3 .

standards showed a good linear relationship between the normalized peak integrals and concentration in the range tested (Figure S2). The spectrum of the filtrate showed only one peak which resonated 0.5 ppm upfield compared to aqueous standards of both AlCl_3 and $\text{Al}(\text{NO}_3)_3$. These similarities indicate that Al leached from the zeolite is octahedrally coordinated, as tetrahedral Al resonates much further upfield, at 40–60 ppm.³⁶ In addition, the Al concentration calculated using the calibration curves for AlCl_3 and $\text{Al}(\text{NO}_3)_3$ was 80.5 ppm, which is comparable to the value obtained from ICP-MS (86.1 ppm). Only highly mobile Al species are detected by liquid-phase NMR, and therefore, colloidal fragments were not significant. These results further support that leaching occurs through homogeneous dissolution and that zeolite fragments do not contribute significantly to the species in solution.

NMR results and the similarities between X-ray diffractograms before and after reaction (Figure 3) suggest that dissolution is either a continuous process that takes place at the crystal's outer surface, or a time-limited process that only involves amorphous material in the sample. To address this question, ZSM-5 was hydrothermally treated five successive times at 170 °C for 90 min in NaCl-saturated solutions at pH 2.5 and leaching was quantified by ICP-MS after each run (Supporting Information). The concentration of Al in solution dropped to 2.5 ppm after the third treatment and further decreased to 0.7 ppm after the last run (Figure S3). The total amount of leached Al over the five successive runs was 3.3 mg or ~4.5% of the aluminum initially present in the catalyst. XRD performed after the last treatment (i.e., 7.5 h at 170 °C) showed no significant loss in crystallinity (Figure S4). Therefore, it appears that NaCl enhances the dissolution of amorphous extra-framework aluminum species but has no significant effect on the MFI lattice. Tests performed on ZSM-5 samples with different elemental compositions further confirmed that NaCl promotes different effects than those involved in hydrothermal dealumination (in pure water).^{7,12} In contrast to previous studies, the Al concentration in solution increased with the Al content of the zeolite (Table S2, Figure S3). Finally, it is worth noting that the repeated treatments did not fully stabilize the samples. Significant leaching (70 ppm Al) was still observed when testing the catalytic activity of the ZSM-5 treated five successive times in HCl/NaCl (Entry 10), which suggest that the organic reactants and/or reaction products also play an active role in the leaching process.

The effect of salts on the dissolution of minerals is well-documented in geochemistry.^{14,15,37} It has been demonstrated that cationic solutes (Na^+ , K^+ , Ca^{2+} , Mg^{2+}) can enhance the dissolution of silica, tectosilicates, and aluminosilicates by up to 100 times.¹⁵ Zeolites, independently of their elemental composition, are tectosilicates. Therefore, salts naturally present in biomass are expected to impact the long-term stability of zeolite catalysts for reactions in the condensed phase. More work is required to fully understand salt effects under reaction conditions, when organic compounds are also present in the reaction medium. However, the theory developed by Dove et al. for the dissolution of silica and feldspars provides solid foundations to guide future research.¹⁵ For example, we observed that NaCl in low concentration (0.07–0.18% (w/w) in water, which corresponds to 1.4–3.6% (w/w) relative to glucose, i.e., similar salt concentration as in dry biomass) enhances dissolution rates significantly more than saturated NaCl solutions (Table 1, Entries 7, 8, and 5), in good agreement with experiments performed on feldspars.^{14,37} The theory developed by Dove et al. also predicts that dissolution rates depend on electrolyte composition and crystal structure, which explains that (i) the stability of the catalyst varied with both NaCl and HCl (Figure 1), and that (ii) primarily amorphous/defective phase in the sample dissolved, even after five successive treatments (Figure S4).

In summary, we demonstrated that salts naturally present in biomass significantly impact the hydrothermal stability of zeolite catalysts, even when highly diluted. The crystalline fraction of the catalyst remained intact. However, Si–O–Al bonds involved in extra-framework species and/or at defect sites underwent a hydrolytic attack, thus leaching Si and Al species into the reaction medium.²⁷ Al NMR demonstrated that Al in solution was octahedrally coordinated, most probably as solvated Al^{3+} ions. These species were active in the isomerization of glucose to fructose, and a linear correlation was found between glucose conversion and Al in solution. This work reveals that future catalyst stability tests have to be performed under relevant biomass conversion conditions.

■ ASSOCIATED CONTENT

Supporting Information

The Supporting Information is available free of charge on the ACS Publications website at DOI: 10.1021/acscatal.5b00888.

Detailed experimental procedures, ICP-MS and XRD results for ZSM-5 after repeated hydrothermal tests, calibration curves, and additional NMR spectra for standard solutions of AlCl_3 and $\text{Al}(\text{NO}_3)_3$ (PDF)

■ AUTHOR INFORMATION

Corresponding Author

*E-mail: tesso@iastate.edu. Phone: +1 515-294-4595.

Author Contributions

[§]These authors contributed equally to this work (D.W.G., J.H., and T.C.H.).

Notes

The authors declare no competing financial interest.

■ ACKNOWLEDGMENTS

This material is based upon work supported in part by Iowa State University, the National Science Foundation under Grant Numbers EEC-0813570 and EPSC-1101284, and the Iowa Energy Center under IEC Grant Number 13-01.

■ REFERENCES

- (1) Xiong, H.; Pham, H. N.; Datye, A. K. *Green Chem.* **2014**, *16*, 4627–4643.
- (2) Jacobs, P. A.; Dusselier, M.; Sels, B. F. *Angew. Chem., Int. Ed.* **2014**, *53*, 8621–8626.
- (3) Matthiesen, J.; Hoff, T.; Liu, C.; Puschel, C.; Rao, R.; Tessonier, J.-P. *Chin. J. Catal.* **2014**, *35*, 842–855.
- (4) Pham, H. N.; Anderson, A. E.; Johnson, R. L.; Schmidt-Rohr, K.; Datye, A. K. *Angew. Chem., Int. Ed.* **2012**, *51*, 13163–13167.
- (5) Ravenelle, R. M.; Copeland, J. R.; Kim, W.-G.; Crittenden, J. C.; Sievers, C. *ACS Catal.* **2011**, *1*, 552–561.
- (6) Pollock, R. A.; Gor, G. Y.; Walsh, B. R.; Fry, J.; Ghampson, I. T.; Melnichenko, Y. B.; Kaiser, H.; DeSisto, W. J.; Wheeler, M. C.; Frederick, B. G. *J. Phys. Chem. C* **2012**, *116*, 22802–22814.
- (7) Ravenelle, R. M.; Schüßler, F.; D'Amico, A.; Danilina, N.; van Bokhoven, J. A.; Lercher, J. A.; Jones, C. W.; Sievers, C. *J. Phys. Chem. C* **2010**, *114*, 19582–19595.
- (8) Kruger, J. S.; Nikolakis, V.; Vlachos, D. G. *Appl. Catal., A* **2014**, *469*, 116–123.
- (9) Kruger, J. S.; Choudhary, V.; Nikolakis, V.; Vlachos, D. G. *ACS Catal.* **2013**, *3*, 1279–1291.
- (10) Gounder, R. *Catal. Sci. Technol.* **2014**, *4*, 2877–2886.
- (11) Okuhara, T. *Chem. Rev.* **2002**, *102*, 3641–3666.
- (12) Ennaert, T.; Geboers, J.; Gobechiya, E.; Courtin, C. M.; Kurttepel, M.; Houthoofd, K.; Kirschhock, C. E. A.; Magusin, P. C. M. M.; Bals, S.; Jacobs, P. A.; Sels, B. F. *ACS Catal.* **2015**, *5*, 754–768.
- (13) Galarneau, A.; Nader, M.; Guenneau, F.; Di Renzo, F.; Gedeon, A. *J. Phys. Chem. C* **2007**, *111*, 8268–8277.
- (14) Icenhower, J. P.; Dove, P. M. *Geochim. Cosmochim. Acta* **2000**, *64*, 4193–4203.
- (15) Dove, P. M.; Han, N.; De Yoreo, J. J. *Proc. Natl. Acad. Sci. U. S. A.* **2005**, *102*, 15357–15362.
- (16) Dove, P. M.; Han, N.; Wallace, A. F.; De Yoreo, J. J. *Proc. Natl. Acad. Sci. U. S. A.* **2008**, *105*, 9903–9908.
- (17) Brown, R. C.; Brown, T. R. *Biorenewable Resources: Engineering New Products from Agriculture*; John Wiley & Sons, Inc: Hoboken, NJ, 2014; pp 92–93.
- (18) Cho, H. J.; Dornath, P.; Fan, W. *ACS Catal.* **2014**, *4*, 2029–2037.
- (19) Lew, C. M.; Rajabbeigi, N.; Tsapatsis, M. *Microporous Mesoporous Mater.* **2012**, *153*, 55–58.
- (20) You, S. J.; Park, E. D. *Microporous Mesoporous Mater.* **2014**, *186*, 121–129.
- (21) Dapsens, P. Y.; Mondelli, C.; Jagielski, J.; Hauert, R.; Perez-Ramirez, J. *Catal. Sci. Technol.* **2014**, *4*, 2302–2311.
- (22) Nikolla, E.; Román-Leshkov, Y.; Moliner, M.; Davis, M. E. *ACS Catal.* **2011**, *1*, 408–410.
- (23) Caratzoulas, S.; Davis, M. E.; Gorte, R. J.; Gounder, R.; Lobo, R. F.; Nikolakis, V.; Sandler, S. I.; Snyder, M. A.; Tsapatsis, M.; Vlachos, D. G. *J. Phys. Chem. C* **2014**, *118*, 22815–22833.
- (24) Pagán-Torres, Y. J.; Wang, T.; Gallo, J. M. R.; Shanks, B. H.; Dumesic, J. A. *ACS Catal.* **2012**, *2*, 930–934.
- (25) Wang, T.; Pagán-Torres, Y. J.; Combs, E. J.; Dumesic, J. A.; Shanks, B. H. *Top. Catal.* **2012**, *55*, 657–662.
- (26) Wang, T.; Glasper, J. A.; Shanks, B. H. *Appl. Catal., A* **2015**, *498*, 214–221.
- (27) Combs, E.; Cinlar, B.; Pagan-Torres, Y.; Dumesic, J. A.; Shanks, B. H. *Catal. Commun.* **2013**, *30*, 1–4.
- (28) Yang, Y.; Hu, C.-W.; Abu-Omar, M. M. *Green Chem.* **2012**, *14*, 509–513.
- (29) Wang, T.; Nolte, M. W.; Shanks, B. H. *Green Chem.* **2014**, *16*, 548–572.
- (30) Rivalier, P.; Duhamet, J.; Moreau, C.; Durand, R. *Catal. Today* **1995**, *24*, 165–171.
- (31) Ravenelle, R. M.; Diallo, F. Z.; Crittenden, J. C.; Sievers, C. *ChemCatChem* **2012**, *4*, 492–494.
- (32) Saha, B.; Abu-Omar, M. M. *Green Chem.* **2014**, *16*, 24–38.
- (33) Li, S.; Tuan, V. A.; Falconer, J. L.; Noble, R. D. *J. Membr. Sci.* **2001**, *191*, 53–59.

(34) Jae, J.; Tompsett, G. A.; Foster, A. J.; Hammond, K. D.; Auerbach, S. M.; Lobo, R. F.; Huber, G. W. *J. Catal.* **2011**, *279*, 257–268.

(35) Mayes, H. B.; Nolte, M. W.; Beckham, G. T.; Shanks, B. H.; Broadbelt, L. J. *ACS Catal.* **2015**, *5*, 192–202.

(36) Fyfe, C. A.; Bretherton, J. L.; Lam, L. Y. *J. Am. Chem. Soc.* **2001**, *123*, 5285–5291.

(37) Stillings, L. L.; Brantley, S. L. *Geochim. Cosmochim. Acta* **1995**, *59*, 1483–1496.